Journal of Hazardous Materials 188 (2011) 334–340

Contents lists available at ScienceDirect

Journal of Hazardous Materials

journal homepage: www.elsevier.com/locate/jhazmat

Barrier properties of poly(vinyl alcohol) membranes containing carbon nanotubes or activated carbon

Erin M. Surdo[a], Iftheker A. Khan[b], Atif A. Choudhury[c], Navid B. Saleh[b], William A. Arnold[a,*]

[a] Department of Civil Engineering, University of Minnesota, 500 Pillsbury Drive Southeast, Minneapolis, MN 55455, United States
[b] Department of Civil and Environmental Engineering, University of South Carolina, 300 Main Street, Columbia, SC 29208, United States
[c] Center for Medicine, Health, and Society, Vanderbilt University, 2301 Vanderbilt Place, Nashville, TN 37235, United States

ARTICLE INFO

Article history:
Received 1 November 2010
Received in revised form 10 January 2011
Accepted 28 January 2011
Available online 4 February 2011

Keywords:
Barrier membrane
Sorption
Diffusion
Sediment cap
Landfill liner
Activated carbon
Carbon nanotubes

ABSTRACT

Carbon nanotube addition has been shown to improve the mechanical properties of some polymers. Because of their unique adsorptive properties, carbon nanotubes may also improve the barrier performance of polymers used in contaminant containment. This study compares the barrier performance of poly(vinyl alcohol) (PVA) membranes containing single-walled carbon nanotubes (SWCNTs) to that for PVA containing powdered activated carbon (PAC). Raw and surface-functionalized versions of each sorbent were tested for their abilities to adsorb 1,2,4-trichlorobenzene and Cu^{2+}, representing the important hydrophobic organic and heavy metal contaminant classes, as they diffused across the PVA. In both cases, PAC (for 1,2,4-trichlorobenzene) and functionalized PAC (for Cu^{2+}) outperformed SWCNTs on a *per mass* basis by trapping more of the contaminants within the barrier membrane. Kinetics of sorption are important in evaluating barrier properties, and poor performance of SWCNT-containing membranes as 1,2,4-TCB barriers is attributed to kinetic limitations.

1. Introduction

The increasing use of carbon nanotubes (CNTs) in research and industry has captured the attention of the environmental community. While risks associated with CNT release to the environment may be a cause for concern [1–3], some argue that the potential benefits afforded by CNT use in environmental engineering applications also deserves research exploration [4,5]. One proposed use of CNTs is adsorption of trace organic contaminants, such as trihalomethanes, substituted benzenes, and polycyclic aromatic hydrocarbons, from water [6–14]. Researchers have also investigated CNTs as a solid-phase extraction medium for organic compounds [5,13,14].

Polymer membranes are used as physical barriers against environmental contamination in a wide variety of applications (landfill liners, silt screens, vapor intrusion barriers, etc.). Powdered activated carbon (PAC) has been shown to slow the diffusion of hydrophobic solutes through high-density polyethylene (HDPE) and HDPE sandwich membranes [15,16]. The added sorbent material traps hydrophobic solutes as they dissolve in the polymer and diffuse across the barrier membrane, resulting in either an increased time to contaminant breakthrough [15] or a reduced contaminant flux [16]. Because CNTs also have high sorption capacities for hydrophobic organic contaminants, we hypothesize that CNT-containing PVA membranes will also improve barrier performance compared with pure polymers.

Beyond the fields of environmental chemistry and engineering, the electrical, mechanical, and thermal properties of CNTs have been studied [17–19]. For example, poly(vinyl alcohol) (PVA) membranes containing CNTs show improved thermal and mechanical properties compared to the pure polymer [20–24]. Ciambelli et al. [21] observed an increase in the glass transition temperature when CNTs were added to PVA. CNT–PVA composites exhibit a higher Young's modulus (i.e., stiffness) than pure PVA [23]. Many of the improvements observed with CNT addition are attributed to an increase in crystallinity [23–25].

Polar functional groups are added to the surfaces of CNTs to better incorporate them into the hydrophilic PVA structure and give further mechanical property improvements to the composites [20,21]. Langley and Fairbrother [26] studied several oxidation techniques and discovered that the type and strength of the oxidant affected the type of functional groups added to carbon surfaces. Any type of oxidation, however, decreases the sorptive capacity of CNTs for hydrophobic compounds lacking functional groups that participate in hydrogen bonding [27,28]. Cho et al. [27] observed a 70% reduction in naphthalene sorption to multi-walled carbon nanotubes with 10% surface oxygen compared with raw material. Sorption of non-polar solutes to PAC also decreases with surface

* Corresponding author. Tel.: +1 612 625 8582; fax: +1 612 626 7750.
E-mail addresses: arnol032@umn.edu, arnol032@tc.umn.edu (W.A. Arnold).

0304-3894/$ – see front matter © 2011 Elsevier B.V. All rights reserved.
doi:10.1016/j.jhazmat.2011.01.130

oxidation [29,30]. Addition of oxidative functional groups, however, increases CNT and PAC sorption capacities for heavy metal ions [28,31–33], another important class of environmental contaminants.

The first objective of this work is to examine the effect of adding single-walled carbon nanotubes (SWCNTs) to PVA on the breakthrough behavior of 1,2,4-trichlorobenzene (1,2,4-TCB), a model hydrophobic contaminant. 1,2,4-TCB diffuses easily through PVA [16] and is expected to readily adsorb to PAC and SWCNTs [7,13]. PVA is a hydrophilic polymer that has been used extensively to study reactive barrier films [15,16,34–36]. While PVA is not typically used for containment in the environment, its high permeability when wet allows efficient laboratory study of diffusion across sorbent-containing barrier membranes. Diffusion across PVA membranes containing PAC or SWCNTs is compared to that for pure PVA. The second objective is to examine the barrier performance of PVA membranes containing surface-functionalized SWCNT and PAC (ox-SWCNT and ox-PAC, respectively). Breakthrough of 1,2,4-TCB (representing hydrophobic organic pollutants) and cupric ion (Cu^{2+}, representing metal ions) across these membranes is evaluated. Finally, while a membrane breakthrough experiment provides information on the barrier performance of a particular sorbent-containing membrane, broader conclusions regarding the use of sorbent particles in barrier membranes require additional information. Sorption isotherms and particle characterization were used to understand the sorption capabilities, surface chemistry, and physical microstructure/macrostructure of each sorbent particle used.

2. Experimental

2.1. Materials

PAC (J.T. Baker) and SWCNTs (Short SWNT 90s, 90%, CheapTubes.com) were used as received. Functionalized PAC and SWCNTs were prepared using a saturated ammonium persulfate solution in 1 M sulfuric acid as described by Langley and Fairbrother [26]. Other chemicals and materials used are described in detail in the Supplementary Data (Section S1).

2.2. Particle characterization

Brunauer–Emmett–Teller (BET) specific surface area for each particle type was measured via a three-point nitrogen sorption isotherm using a Quantasorb surface area analyzer (Quantachrome). Sorbent particles were also characterized using high-resolution transmission electron microscopy (HRTEM) and Raman spectroscopy. Scanning electron microscopy (SEM) images of sorbent particle-containing PVA membranes were collected. Sample preparation and imaging methods are described in the Supplementary Data (Section S2).

2.3. Membrane preparation

Sorbent-containing PVA membranes were prepared by sonicating sorbent particles in 15 mL water for 10 min before adding 1.5 g PVA. The particle/PVA suspension was heated (<100 °C) while stirring rapidly for 10 min, cooled, degassed under vacuum, and cast on a polytetrafluoroethylene (PTFE) plate. After drying at room temperature for 2 days, the PVA was crosslinked in a 150 °C oven for 1 h. Thicknesses of hydrated membranes were measured with a micrometer (Mitutoyo).

2.4. Batch sorption, batch uptake, and diaphragm cell breakthrough experiments

All 1,2,4-TCB experiments were conducted in nanopure water. Cu^{2+} experiments were conducted in pH 7.2 50 mM Tris buffer (7.88 g/L TRIZMA–HCl; 0.18 g/L NaOH; 5.85 g/L NaCl). Batch experiment initial concentrations and breakthrough experiment upstream concentrations were 50 μM and 1 mM for all 1,2,4-TCB and Cu^{2+} experiments, respectively.

Equilibrium experiments were conducted for particles and membranes. For each isotherm, a series of vials was loaded with particles or dry membrane pieces with varying mass. Vials were filled with liquid medium, and membranes were allowed to hydrate overnight before spiking with a concentrated stock solution to achieve the desired initial concentration. Vials containing particles were placed on a rotator or hand-shaken twice daily for at least 6 days prior to sampling. Cu^{2+} samples (100 μL) were filtered with a 0.22 μm nylon syringe filter (Acrodisc). 1,2,4-TCB samples (250 μL) were collected after either centrifugation at 900 × *g* for 15 min or allowing particles to settle for 48 h. Membrane partitioning/isotherm experiments were stored on a shaker table for at least 24 and 5 days for 1,2,4-TCB and Cu^{2+} experiments, respectively, before collecting 250-μL and 100-μL samples from each.

Batch uptake experiments were conducted by placing equal-mass pieces of dry membrane into a series of vials and adding the appropriate liquid medium. After overnight hydration, each vial was spiked with concentrated stock solution. Samples were collected from one vial at each time point. Sample volumes were equivalent to those for equilibrium experiments.

Breakthrough experiments were conducted by placing hydrated membranes between two diaphragm cells [15,16], filling the cells with the appropriate liquid medium, and sealing the joint with epoxy. The upstream cell (representing the contaminated medium to be contained) was spiked with either a concentrated 1,2,4-TCB stock solution in acetone or a concentrated cupric chloride solution in Tris buffer to achieve the desired initial upstream concentration. Samples (500 μL) were collected from the downstream cell (the initially uncontaminated side of the system) throughout each experiment as the contaminants diffused through the membrane. The sample volume was replaced with clean liquid medium to maintain a constant downstream volume. Cu^{2+} experiment upstream samples were also collected in this manner. Fifty-microliter samples were collected from 1,2,4-TCB experiment upstream cells without replacement. All samples were extracted (if necessary) and analyzed as described in the Supplementary Data (Section S3).

3. Results

3.1. Particle characterization

Table 1 lists BET specific surface areas for each sorbent particle type. Other researchers have compared BET specific surface areas for raw and functionalized particles with mixed results – some observed increases in surface area upon oxidation [8] and others have observed surface area reduction [10,31].

SEM and TEM images of membranes and free particles, respectively, are shown in Fig. 1. The inset of Fig. 1c clearly shows bundled raw SWCNTs (~40 nm), whereas relative debundling (to ~20 nm) and shortening of the SWCNTs are clearly visible on the TEM image presented as an inset in Fig. 1d for ox-SWCNTs. SEM images for PVA membranes containing SWCNTs (Fig. 1c) shows randomly organized SWCNTs in the PVA matrix compared to clearly aligned ox-SWCNTs (Fig. 1d). The direction of alignment for the oxidized SWCNTs is parallel to the direction of diffusion through the mem-

Table 1
Surface area and Langmuir fit parameters for various sorbent types.[a]

Sorbent type	BET specific surface area (m^2/g)	Solute	q_{max} (μmol/g)	b (L/μmol)
PAC	1100 ± 90	1,2,4-TCB	3600 ± 500	2 ± 1
		Cu^{2+}	300 ± 20	0.003 ± 0.001
SWCNT	380 ± 10	1,2,4-TCB	2600 ± 800	0.04 ± 0.02
ox-PAC	700 ± 100	1,2,4-TCB	1200 ± 300	0.04 ± 0.02
		Cu^{2+}	3000 ± 1000	0.02 ± 0.02
ox-SWCNT	440 ± 40	1,2,4-TCB	1800 ± 900	0.04 ± 0.03
		Cu^{2+}	630 ± 70	0.04 ± 0.04

[a] Errors given are 95% confidence intervals.

brane when mounted in the diaphragm cell. While flakes or other impermeable obstructions aligned perpendicular to the direction of diffusion can reduce membrane permeability [37], parallel alignment does not physically affect contaminant flux.

Raman spectra were used to estimate SWCNT diameters of 1.1–1.5 nm [38,39]. Differences in spectra for raw and functionalized SWCNTs indicate an increase in defect level as expected with the addition of functional groups [40]. The Raman spectra for raw and functionalized PAC are consistent with those reported previously [41,42]; i.e., characteristic peaks at 1321 and 1588 cm^{-1} and trough deepening (at ~1480 cm^{-1}) were observed for functionalized PAC.

3.2. Sorption isotherms

Sorption isotherm data for free particles were collected and fit to the Langmuir isotherm using the least-squares fitting option in Scientist for Windows (MicroMath):

$$q = \frac{q_{max} bC}{1 + bC} \quad (1)$$

where q (μmol/g) is the sorbed solute concentration, q_{max} (μmol/g) is the total capacity of the sorbent for solute sorption, C (μM) is the concentration of solute in solution at equilibrium, and b (L/μmol) is a fitting parameter. Resulting fit parameters are given in Table 1.

Isotherm experiments using pure and sorbent-containing PVA membranes were also conducted, though the scatter present in the data makes quantitative conclusions difficult. Generally, the observed sorption capacities of the membrane-bound sorbent particles were lower than expected based on the free particle results.

3.3. Breakthrough curves

Normalized breakthrough curves obtained from diaphragm cell experiments for 1,2,4-TCB and Cu^{2+} diffusion across pure PVA and PVA membranes containing sorbent particles are shown in Figs. 2 and 3, respectively. The slope of each curve is equivalent to the permeability of the membrane, according to Eq. (2) [43,44]:

$$\frac{C_{down} V_{down}}{C_{up} AL} = \frac{P}{L^2}(t - t_{lag}) \quad (2)$$

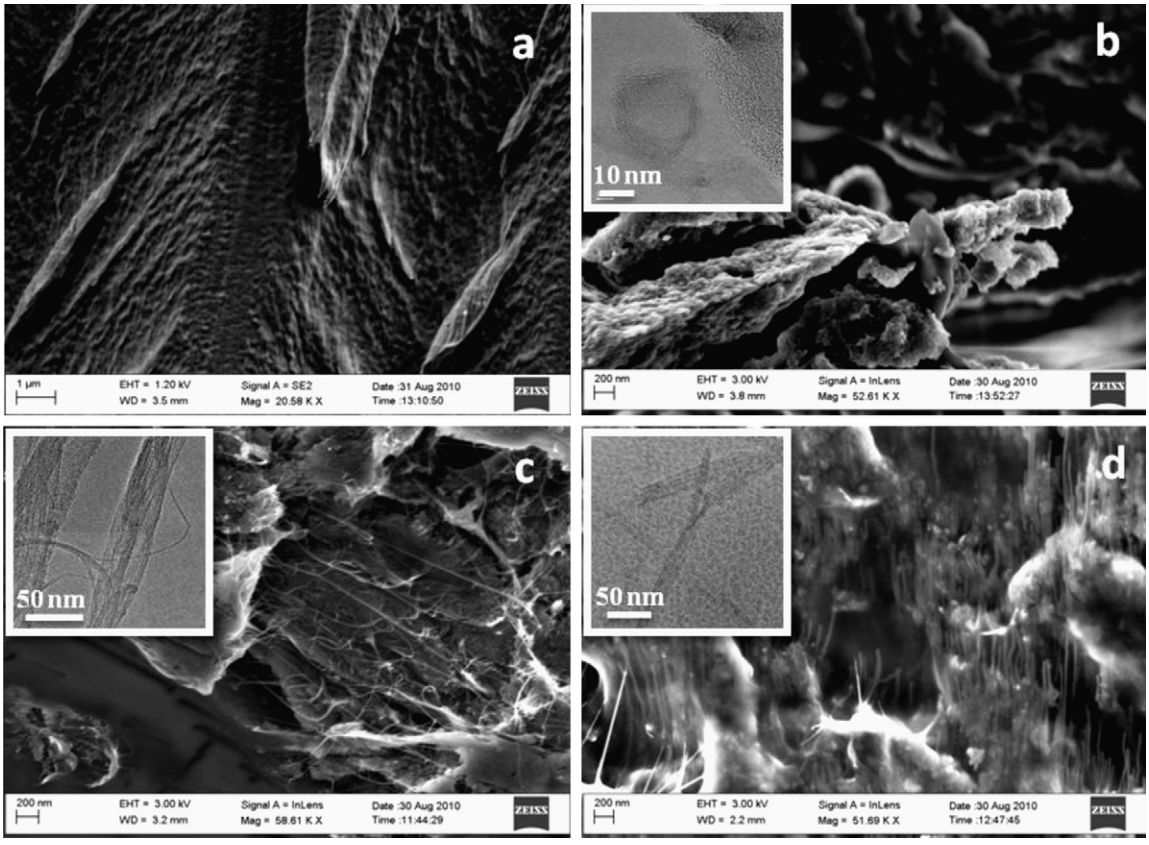

Fig. 1. FESEM micrographs of PVA (a), PVA with ox-PAC (b), PVA with SWCNT (c), and PVA with ox-SWCNT (d). Inset shows HRTEM micrographs of ox-PAC (b), SWCNT (c), and ox-SWCNT (d).

Table 2
Breakthrough and uptake experiment summary[a].

Solute	Sorbent	C_{s0} (g/L)[b]	L (μm)	C_{up} (μM)	$P \times 10^{12}$ (m^2/s)	t_{lag} (h)	PVA t_{lag} (h)[c]	Relative k_1 (s^{-1})	Relative k_2 ($\mu M^{-1}\ s^{-1}$)	Relative Φ
TCB	–	–	186 ± 5	52 ± 1	63 ± 3	0.1 ± 0.6	–	–	–	–
TCB	–	–	222 ± 5	47 ± 3	94 ± 8	0 ± 2	–	–	–	–
TCB	PAC	32	168 ± 4	44 ± 5	140 ± 20	2 ± 1	0.10	4.8×10^{-6}	4.2×10^{-11}	0.011
TCB	PAC[d]	69	270 ± 20	44 ± 2	11 ± 1	51 ± 7	0.3	1.0×10^{-5}		0.061
				53 ± 2	40 ± 4	370 ± 50				
TCB	SWCNT	77	250 ± 10	48 ± 6	68 ± 10	14 ± 5	0.2	9.0×10^{-7}	4.5×10^{-12}	0.005
TCB	SWCNT	141	126 ± 6	48 ± 4	140 ± 20	0.8 ± 0.6	0.06	1.6×10^{-6}		0.002
TCB	ox-PAC	62	222 ± 5	48 ± 4	70 ± 9	6 ± 6	0.2	–	–	–
TCB	ox-SWCNT	42	227 ± 6	48 ± 2	82 ± 8	−2 ± 5[e]	0.2	–	–	–
Cu^{2+}	–	–	230 ± 10	1220 ± 10	8.7 ± 0.5	0.4 ± 0.3	–	–	–	–
Cu^{2+}	–	–	328 ± 8	1260 ± 20	7.5 ± 0.2	1.0 ± 0.2	–	–	–	–
Cu^{2+}	PAC	147	296 ± 6	970 ± 20	19.1 ± 0.6	0.5 ± 0.2	0.8	–	–	–
Cu^{2+}	ox-PAC	186	230 ± 3	970 ± 10	5.5 ± 0.2	77 ± 3	0.5	3.0×10^{-5}	5.2×10^{-11}	0.298
Cu^{2+}	ox-SWCNT	157	85 ± 4	998 ± 9	5.5 ± 0.2	5.4 ± 0.2	0.06	3.0×10^{-5}	3.0×10^{-10}	0.040

[a] Errors given are 95% confidence intervals.
[b] C_{s0} is the sorbent content per membrane volume.
[c] PVA t_{lag} is a predicted value for pure PVA with the same thickness as the membrane studied.
[d] 1,2,4-TCB breakthrough across PAC-containing PVA occurred in three distinct phases: (1) the lag time, (2) a period of low apparent permeability, and (3) a period with permeability similar to that observed for pure PVA. The two rows of information given are the result of applying Eq. (2) to data in the latter two phases.
[e] A negative lag time is not possible theoretically, but is the result of errors associated with extrapolating an x-intercept from a linear regression. In this case, a very small lag time with a large margin of error led to the perception of a negative value.

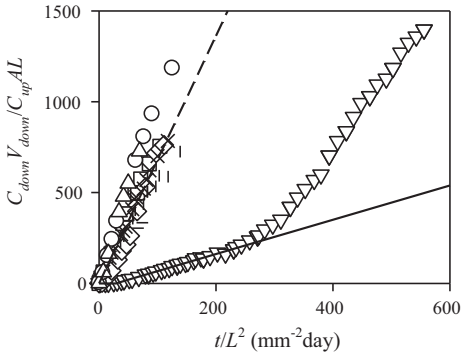

Fig. 2. Normalized 1,2,4-TCB breakthrough curves from diagphram cell experiments for pure PVA (-, □), PVA with 32 (△) or 69 g/L PAC (▽), PVA with 77 (◊) or 141 g/L SWCNT (○), PVA with 62 g/L ox-PAC (|), and PVA with 42 g/L ox-SWCNT (×). The solid line (—) indicates a linearized breakthrough curve corresponding to the initial flux across the membrane containing 69 g/L PAC, which is significantly reduced compared to that predicted for diffusion across pure PVA (dashed curve – –).

where C_{down} (μM) and C_{up} (μM) are the downstream and upstream aqueous concentrations, V_{down} (m^3) is the volume of the downstream cell, A (m^2) and L (m) are the area and thickness of the membrane, P (m^2/s) is the permeability, which is the product of the diffusion coefficient, D, and the membrane–water partition coefficient, t (s) is time, and t_{lag} (s) is the lag time, or the time it takes for a contaminant to reach the downstream side of an initially contaminant-free membrane. Eq. (2) was derived using Fick's law and a set of simplifications associated with thin film diffusion [43,44]. Permeabilities, observed lag times, and other experimental information are in Table 2.

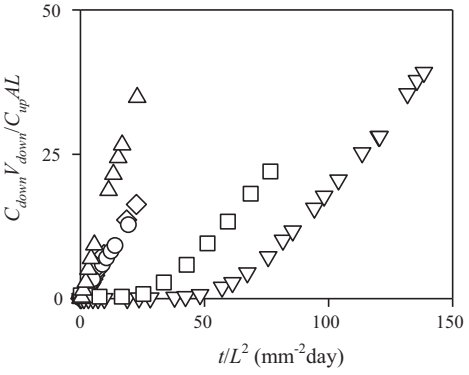

Fig. 3. Normalized Cu^{2+} breakthrough curves from diaphragm cell experiments for pure PVA (○,◊), PVA with 147 g/L PAC (△), PVA with 186 g/L ox-PAC (▽), and PVA with 157 g/L ox-SWCNT (□).

3.4. Membrane uptake curves

Differences in the rates of contaminant uptake by membrane-bound particles were also investigated. Fig. 4 presents normalized pseudo-first-order uptake data as measured by concentration loss in aqueous solution.

4. Discussion

4.1. Sorption mechanisms

The isotherms described in Table 1 provide insight into the interactions between solutes and the embedded sorbent particles and allow interpretation of membrane breakthrough data. Oxidation with persulfate results in a high concentration of surface carboxylic acid groups [26]. Cu^{2+} forms both inner sphere and outer sphere complexes with carboxylic acid groups [28]. This electrostatic attraction ceases when enough Cu^{2+} molecules are present to neutralize the surface, leading to a plateau at q_{max} for both ox-PAC and ox-SWCNT.

The π–π interactions thought to drive the aromatic sorption to CNTs are best described by a monolayer Langmuir sorption isotherm model [6]. Hydrophobic interactions, however, may allow for the weak adsorption of additional layers, leading to the Freundlich isotherms reported by many researchers studying aromatic sorption to CNTs [7,12,13,45]. Langmuir fits were used in this study because they captured the data and because Langmuir fit parameters are required for use in the diffusion models described below.

4.2. Factors controlling 1,2,4-TCB sorption and diffusion in PVA

The most direct method of studying barrier properties of sorbent-containing membranes is to compare their breakthrough curves to those for pure polymers (Fig. 2). The PVA membrane with 69 g/L PAC was the only sorbent-containing membrane with

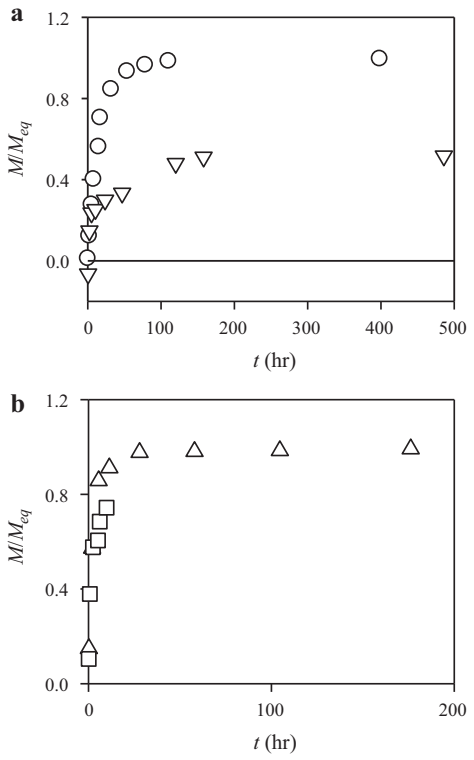

Fig. 4. Membrane uptake plots for 1,2,4-TCB (a) and Cu^{2+} (b) by PVA membranes containing 32 g/L PAC (○), 77 g/L SWCNT (▽), 186 g/L ox-PAC (△), and 157 g/L ox-SWCNT (□). M is the sorbed contaminant mass and M_{eq} is the expected mass sorbed to the membrane-bound particles at equilibrium (based on the equilibrium isotherms for free particles described in Table 1).

a measurably different 1,2,4-TCB permeability than the pure polymer. The effect was not an increased time to breakthrough (t_{lag}), but a reduced steady-state flux. Fast "reaction" relative to diffusion results in increased lag times observed previously [34]. Slower "reaction" can lead to reduced flux [16].

The relative rates of reaction and diffusion can be described using the Damköhler number, Φ:

$$\Phi = \frac{k_1 L^2}{D} \quad (3)$$

where k_1 is a pseudo-first-order "reaction" rate constant. The relative kinetic differences between 1,2,4-TCB sorption to PVA-encapsulated PAC and SWCNTs have been captured in the uptake experiments described in Fig. 4a. Assuming pseudo-first-order sorption kinetics, plotting ln C versus t allows estimation of the relative pseudo-first-order rate constants, k_1, for each sorbent type (Table 2). Because diffusion also plays a part in these membrane-based uptake experiments, k_1 determined using this method is not an actual sorption rate constant. The relative differences between k_1 derived from PAC and SWCNT data, however, provide useful information.

Relative second-order rate constants, k_2, are also given in Table 2:

$$k_2 = \frac{k_1}{C_{s0} q_{max}} \quad (4)$$

where C_{s0} is the sorbent loading in the membrane and the product, $C_{s0}q_{max}$, is the sorptive capacity per membrane volume. The value may be doubled for uptake of 1,2,4-TCB by membrane-bound SWCNTs if the reduction in capacity observed in Fig. 4a is also considered.

Typically, Damköhler numbers should be above 0.01 for any visible barrier improvements with the addition of an active scavenger and above 100 to show increased lag time-type behavior [46]. The values in Table 2 are relative numbers based on relative kinetic data, however, so the absolute values of Φ reported in Table 2 cannot be compared to this theoretical range. Because Φ for the membrane with 69 g/L PAC was more than 5 times greater than for the rest of the 1,2,4-TCB breakthrough experiments, we suspect that kinetics are the reason this sorptive membrane showed barrier improvements (i.e., a reduced permeability) while the others did not. (A reduced sorbent loading and a thinner membrane contributed to the low Damköhler number for the membrane with 32 g/L PAC.)

There are several possible explanations for the slow rate of 1,2,4-TCB sorption to membrane-bound SWCNTs. The rate of sorption to outer surface sites on an uncapped SWCNT cylinder will obviously be faster than the rate of sorption to inner sites. Inner sites are likely inaccessible, especially for bulky compounds like 1,2,4-TCB that must diffuse through the tube end (1.1–1.5 nm diameter) to access the inner surface sites. (The LeBas molar volume of aqueous 1,2,4-TCB is 147.6 cm^3/mol [47], yielding a diameter of 0.78 nm using a spherical assumption). In fact, the M_{eq} values in Fig. 4a were calculated for the uptake experiments using the free solution sorption isotherms parameters listed in Table 1. The leveling of the SWCNT data in Fig. 4a at $M/M_{eq} = 0.5$ indicates that either 1,2,4-TCB cannot easily access the inner surfaces (half of the total surface area) when embedded in PVA, or that, perhaps more likely, interactions with the polymer material otherwise decrease the sorption capacity. This effect accounts for a two-fold difference in sorption rate, but the observed second-order sorption rate constants for PAC and SWCNT differ by a factor of 10. Tight bundling of SWCNTs may also impede 1,2,4-TCB access to some outer SWCNT surfaces, slowing sorption to the interstitial surfaces. Zhang et al. [48] observed reduced sorption capacities in water and attributed the results to aggregation of SWCNTs. Local aggregation may also contribute to early breakthrough and/or leakage of 1,2,4-TCB in breakthrough experiments by creating areas of heightened and reduced sorbent content in the membrane. The SEM images shown in Fig. 1 support an even distribution of particles locally, but variation across the entire area used for diffusion experiments may cause this early leakage effect.

Functional groups intentionally added to PAC and SWCNT surfaces reduced sorption capacities for 1,2,4-TCB (Table 1). This result was expected because functional groups have been shown to reduce the sorption capacity of CNTs for hydrophobic aromatic compounds [48]. Thus, ox-PAC and ox-SWCNT were unsuccessful at quantifiably intercepting 1,2,4-TCB as it diffused across PVA membranes.

Another feature of Fig. 2 worth noting is the observed transition from reduced flux to a steady-state flux (nearly parallel to the pure PVA membrane breakthrough curve) for the membrane containing 69 g/L PAC. This transition occurred after an estimated 37% of the total sorption capacity of the PAC was occupied by 1,2,4-TCB. This PAC efficiency was calculated from the area between the observed breakthrough curve (at reduced flux) and the curve expected for a pure PVA membrane of the same thickness. Somewhat similar PAC efficiencies were observed in sandwich membranes containing PAC [15].

4.3. Factors controlling Cu^{2+} sorption and diffusion in PVA

Larger sorbent loadings were used in Cu^{2+} breakthrough experiments to overcome the generally lower sorption capacity for Cu^{2+}. At the loadings used, increased lag times for membranes with functionalized particles were observed, as shown in Fig. 3. Oxidation substantially increases the capacity for heavy metals sorption [49]. Thus, PAC was not expected to affect Cu^{2+} breakthrough as appreciably as its oxidized counterpart (as shown in Fig. 3), nor were SWCNTs (not tested).

Relative Damköhler numbers were determined for the ox-PAC and ox-SWCNT-containing membranes used for the Cu^{2+} breakthrough experiments (Table 2). Relative Φ for Cu^{2+} cannot be compared with relative Φ for 1,2,4-TCB, because D for Cu^{2+} (5.3×10^{-12} m^2/s) is lower than D for 1,2,4-TCB (1.3×10^{-11} m^2/s). Because of the added influence of membrane diffusion for Cu^{2+}, the k_2 values determined from data in Fig. 4b are even lower than the actual second-order sorption rate constants. If we were to correct all of the relative Φ values in Table 2, the correction factor for the Cu^{2+} values should be larger than the correction factor for the 1,2,4-TCB values. This correction would result in larger Φ values for both Cu^{2+} experiments than for all 1,2,4-TCB experiments. A large Φ explains the lag time-lengthening behavior observed in Cu^{2+} experiments [46].

In previous studies, the performance of reactive or sorbent-containing membranes with respect to slowing contaminant diffusion has been measured by determining the "effective" sorbent loading. Yang et al. [34] developed an expression for the extended lag time based on the theoretical stoichometry of an irreversible reaction, and Warta et al. [36] adapted this expression for use with materials that sorb using the Langmuir isotherm:

$$t_{\text{lag}} = \frac{L^2 C_{s0} q_{\max}}{2DH(C_{\text{up}} - C_e)} \quad (5)$$

where C_e is the aqueous concentration at the shoulder of the Langmuir isotherm, when the capacity of the sorbent is first reached. Effective C_{s0} values calculated from observed lag times using Eq. (5) were 17 and 46 g/L (9 and 29% of the actual C_{s0}) for ox-PAC and ox-SWCNT, respectively, indicating that more of the usable sorptive surface area of the ox-SWCNT was occupied by Cu^{2+} before breakthrough when compared to ox-PAC. Effective C_{s0} is a good measure to consider when comparing cost, because it is used to determine how much of each sorbent is required to achieve the same barrier effect. The faster k_2 value describing sorption to ox-SWCNT may explain the higher percent effectiveness (*per capacity*) of the ox-SWCNT. The ox-PAC, however, was more effective *per mass* because of its higher sorption capacity for Cu^{2+}.

4.4. Implications

While PVA membranes are typically not used as contaminant barriers, PVA was used in this study to provide an easy, side-by-side comparison of sorbents. SWCNT-containing PVA performed poorly compared with PAC-containing PVA when used for 1,2,4-TCB containment. The effectiveness of SWCNTs, however, might be different in an alternative membrane matrix, such as HDPE. Future work on polymer–sorbent interaction using other polymer matrices like HDPE is a must. While other materials may improve the efficiency of SWCNTs, vast improvements in barrier properties with the addition of SWCNTs are unlikely. Future research on sorbent-containing membrane barriers for hydrophobic organics is best focused on using coke, activated carbon, and other less expensive materials with high *per mass* sorption capacities. Future work on membranes amended with activated carbons should include study of the effects of environmental variables like temperature and the presence of impurities (e.g., natural organic matter, other competing sorbates) on the membranes' barrier properties. The success of ox-PAC and ox-SWCNT in trapping Cu^{2+} implies that these sorbents may be useful for the trapping and recovery of heavy metals. In our experiments, however, the ox-PAC performed better on a *per mass* basis than the ox-SWCNT.

Acknowledgements

This work was primarily supported by a Doctoral Dissertation Fellowship awarded to E.M.S. by the Graduate School of the University of Minnesota. Ancillary support came from the Cooperative Institute for Coastal and Estuarine Environmental Technology (CICEET) and the National Science Foundation. We also thank the research group of Professor Andreas Stein for providing training and access to their sonicator, the University of South Carolina Electron Microscopy Center for instrument use and technical assistance, the reviewers for their constructive comments, and Professor Edward Cussler for valuable discussions.

Appendix A. Supplementary data

Supplementary data associated with this article can be found, in the online version, at doi:10.1016/j.jhazmat.2011.01.130.

References

[1] M.R. Wiesner, G.V. Lowry, P. Alvarez, D. Dionysiou, P. Biswas, Assessing the risks of manufactured nanomaterials, Environ. Sci. Technol. 40 (2006) 4336–4345.
[2] C.-w. Lam, J.T. James, R. McCluskey, S. Arepalli, R.L. Hunter, A review of carbon nanotube toxicity and assessment of potential occupational and environmental health risks, Crit. Rev. Toxicol. 36 (2006) 189–217.
[3] E.J. Petersen, R.A. Pinto, P.F. Landrum, J.W.J. Weber, Influence of carbon nanotubes on pyrene bioaccumulation from contaminated soils by earthworms, Environ. Sci. Technol. 43 (2009) 4181–4187.
[4] M.S. Mauter, M. Elimelech, Environmental applications of carbon-based nanomaterials, Environ. Sci. Technol. 42 (2008) 5843–5859.
[5] S. Andreescu, J. Njagi, C. Ispas, M.T. Ravalli, JEM spotlight: applications of advanced nanomaterials for environmental monitoring, J. Environ. Monitor. 11 (2009) 27–40.
[6] R.Q. Long, R.T. Yang, Carbon nanotubes as superior sorbent for dioxin removal, J. Am. Chem. Soc. 123 (2001) 2058–2059.
[7] X. Peng, Y. Li, Z. Luan, Z. Di, H. Wang, B. Tian, Z. Jia, Adsorption of 1,2-dichlorobenzene from water to carbon nanotubes, Chem. Phys. Lett. 376 (2003) 154–158.
[8] C.-J.M. Chin, L.-C. Shih, H.-J. Tsai, T.-K. Liu, Adsorption of o-xylene and p-xylene from water by SWCNTs, Carbon 45 (2007) 1254–1260.
[9] C. Lu, Y.-L. Chung, K.-F. Chang, Adsorption of trihalomethanes from water with carbon nanotubes, Water Res. 39 (2005) 1183–1189.
[10] W. Chen, L. Duan, D. Zhu, Adsorption of polar and nonpolar organic chemicals to carbon nanotubes, Environ. Sci. Technol. 41 (2007) 8295–8300.
[11] K. Yang, L. Zhu, B. Xing, Adsorption of polycyclic aromatic hydrocarbons by carbon nanomaterials, Environ. Sci. Technol. 40 (2006) 1855–1861.
[12] D. Lin, B. Xing, Adsorption of phenolic compounds by carbon nanotubes: role of aromaticity and substitution of hydroxyl groups, Environ. Sci. Technol. 42 (2008) 7254–7259.
[13] G. Liu, J. Wang, Y. Zhu, X. Zhang, Application of multiwalled carbon nanotubes as a solid-phase extraction sorbent for chlorobenzenes, Anal. Lett. 37 (2004) 3085–3104.
[14] M. Asensio-Ramos, J. Hernández-Borges, T.M. Borges-Miquel, M.A. Rodríguez-Delgado, Evaluation of multi-walled carbon nanotubes as solid-phase extraction adsorbents of pesticides from agricultural, ornamental and forestal soils, Anal. Chim. Acta 647 (2009) 167–176.
[15] E.M. Surdo, E.L. Cussler, W.A. Arnold, Sorptive and reactive scavenger-containing sandwich membranes as contaminant barriers, J. Environ. Eng. 135 (2009) 69–76.
[16] E.M. Surdo, E.L. Cussler, P.J. Novak, W.A. Arnold, Geomembranes containing powdered activated carbon have the potential to improve containment of chlorinated aromatic compounds, Environ. Sci. Technol. 43 (2009) 8916–8922.
[17] M.M.J. Treacy, T.W. Ebbesen, J.M. Gibson, Exceptionally high Young's modulus observed for individual carbon nanotubes, Nature 381 (1996) 678–680.
[18] A.B. Dalton, S. Collins, E. Munoz, J.M. Razal, V.H. Ebron, J.P. Ferraris, J.N. Coleman, B.G. Kim, R.H. Baughman, Super-tough carbon-nanotube fibres, Nature 423 (2003) 703.
[19] A.B. Dalton, S. Collins, J. Razal, E. Munoz, V.H. Ebron, B.G. Kim, J.N. Coleman, J.P. Ferraris, R.H. Baughman, Continuous carbon nanotube composite fibers: properties, potential applications, and problems, J. Mater. Chem. 14 (2004) 1–3.
[20] M.S.P. Shaffer, A.H. Windle, Fabrication and characterization of carbon nanotube/poly(vinyl alcohol) composites, Adv. Mater. 11 (1999) 937–941.
[21] P. Ciambelli, M. Sarno, G. Gorrasi, D. Sannino, M. Tortora, V. Vittoria, Preparation and physical properties of carbon nanotubes-PVA nanocomposites, J. Macromol. Sci. Phys. 44 (2005) 779–795.
[22] W. Ni, B. Wang, H. Wang, Y. Zhang, Fabrication and properties of carbon nanotube and poly(vinyl alcohol) composites, J. Macromol. Sci. B 45 (2006) 659–664.
[23] K.P. Ryan, M. Cadek, V. Nicolosi, D. Blond, M. Ruether, G. Armstrong, H. Swan, A. Fonseca, J.B. Nagy, W.K. Maser, W.J. Blau, J.N. Coleman, Carbon nanotubes for reinforcement of plastics? A case study with poly(vinyl alcohol), Compos. Sci. Technol. 67 (2007) 1640–1649.
[24] J.N. Coleman, M. Cadek, K.P. Ryan, A. Fonseca, J.B. Nagy, W.J. Blau, M.S. Ferreira, Reinforcement of polymers with carbon nanotubes. The role of an ordered

polymer interfacial region. Experiment and modeling, Polymer 47 (2006) 8556–8561.
[25] O. Probst, E.M. Moore, D.E. Resasco, B.P. Grady, Nucleation of polyvinyl alcohol crystallization by single-walled carbon nanotubes, Polymer 45 (2004) 4437–4443.
[26] L.A. Langley, D.H. Fairbrother, Effect of wet chemical treatments on the distribution of surface oxides on carbonaceous materials, Carbon 45 (2007) 47–54.
[27] H.-H. Cho, B.A. Smith, J.D. Wnuk, D.H. Fairbrother, W.P. Ball, Influence of surface oxides on the adsorption of naphthalene onto multiwalled carbon nanotubes, Environ. Sci. Technol. 42 (2008) 2899–2905.
[28] G.-C. Chen, X.-Q. Shan, Y.-S. Wang, Z.-G. Pei, X.-E. Shen, B. Wen, G. Owens, Effects of copper, lead, and cadmium on the sorption and desorption of atrazine onto and from carbon nanotubes, Environ. Sci. Technol. 42 (2008) 8297–8302.
[29] T. Karanfil, J.E. Kilduff, Role of granular activated carbon surface chemistry on the adsorption of organic compounds. 1. Priority pollutants, Environ. Sci. Technol. 33 (1999) 3217–3224.
[30] I.I. Salame, T.J. Bandosz, Role of surface chemistry in adsorption of phenol on activated carbons, J. Colloid Interf. Sci. 264 (2003) 307–312.
[31] G. Andrade-Espinosa, E. Muñoz-Sandoval, M. Terrones, M. Endo, H. Terrones, J.R. Rangel-Mendez, Acid modified bamboo-type carbon nanotubes and cup-stacked-type carbon nanofibres as adsorbent materials: cadmium removal from aqueous solution, J. Chem. Technol. Biot. 84 (2009) 519–524.
[32] M. Goyal, V.K. Rattan, D. Aggarwal, R.C. Bansal, Removal of copper from aqueous solutions by adsorption on activated carbons, Colloid. Surface. A 190 (2001) 229–238.
[33] D.-M. Zhou, Y.-J. Wang, H.-W. Wang, S.-Q. Wang, J.-M. Cheng, Surface-modified nanoscale carbon black used as sorbents for Cu(II) and Cd(II), J. Hazard. Mater. 174 (2009) 34–39.
[34] C. Yang, E.E. Nuxoll, E.L. Cussler, Reactive barrier films, AIChE J. 47 (2001) 295–302.
[35] E.E. Nuxoll, E.L. Cussler, The third parameter in reactive barrier films, AIChE J. 51 (2005) 456–463.
[36] A.M. Warta, W.A. Arnold, E.L. Cussler, Permeable membranes containing crystalline silicotitanate as model barriers for cesium ion, Environ. Sci. Technol. 39 (2005) 9738–9743.
[37] E.L. Cussler, S.E. Hughes, W.J. Ward III, R. Aris, Barrier membranes, J. Membr. Sci. 38 (1988) 161–174.
[38] N.B. Saleh, L.D. Pfefferle, M. Elimelech, Aggregation kinetics of multiwalled carbon nanotubes in aquatic systems: Measurements and environmental implications, Environ. Sci. Technol. 42 (2008) 7963–7969.
[39] N.B. Saleh, L.D. Pfefferle, M. Elimelech, Influence of biomacromolecules and humic acid on the aggregation kinetics of single-walled carbon nanotubes, Environ. Sci. Technol. 44 (2010) 2412–2418.
[40] M. Bockrath, W. Liang, D. Bozovic, J.H. Hafner, C.M. Lieber, M. Tinkham, H. Park, Resonant electron scattering by defects in single-walled carbon nanotubes, Science 291 (2001) 283–285.
[41] N. Shimodaira, A. Masui, Raman spectroscopic investigations of activated carbon materials, J. Appl. Phys. 92 (2002) 902–909.
[42] M. Koh, T. Nakajima, Adsorption of aromatic compounds on C_xN-coated activated carbon, Carbon 38 (2000) 1947–1954.
[43] J. Crank, The Mathematics of Diffusion, 2nd ed., Clarendon Press, Oxford, U.K, 1975.
[44] E.L. Cussler, Diffusion: Mass transfer in Fluid Systems, 2nd ed., Cambridge University Press, Cambridge, U.K, 1997.
[45] X. Wang, S. Tao, B. Xing, Sorption and competition of aromatic compounds and humic acid on multiwalled carbon nanotubes, Environ. Sci. Technol. (2009) 6214–6219.
[46] R. DiFelice, D. Cazzola, M. Garbero, P. Ottonello, Unsteady- and steady-state gas permeation through active packaging walls, Packag. Technol. Sci. 21 (2008) 185–191.
[47] R.C. Reid, J.M. Prausnitz, B.E. Polling, Properties of Gases and Liquids, 4th ed., McGraw-Hill, New York, 1987.
[48] S. Zhang, T. Shao, S.S.K. Bekaroglu, T. Karanfil, The impacts of aggregation and surface chemistry of carbon nanotubes on the adsorption of synthetic organic compounds, Environ. Sci. Technol. 43 (2009) 5719–5725.
[49] H.-H. Cho, K. Wepasnick, B.A. Smith, F.K. Bangash, D.H. Fairbrother, W.P. Ball, Sorption of aqueous Zn[II] and Cd[II] by multiwall carbon nanotubes: The relative roles of oxygen-containing functional groups and graphenic carbon, Langmuir 26 (2010) 967–981.